Title

Polarity control during molecular beam epitaxy growth of Mg-doped GaN

Journal

Journal of Vacuum Science & Technology B, 21(4)

ISSN

1071-1023

Authors

Green, D S

Haus, E

Wu, F

et al.

Publication Date

2003-07-01

Peer reviewed

Polarity control during molecular beam epitaxy growth of Mg-doped GaN

D. S. Green
Electrical and Computer Engineering Department, University of California, Santa Barbara, California 93106

E. Haus, F. Wu, and L. Chen
Materials Department, University of California, Santa Barbara, California 93106

U. K. Mishra
Electrical and Computer Engineering Department, University of California, Santa Barbara, California 93106

J. S. Speck[a)]
Materials Department, University of California, Santa Barbara, California 93106

(Received 4 March 2003; accepted 26 April 2003; published 5 August 2003)

Mg doping has been found in some situations to invert growth on Ga-face GaN to N-face. In this study, we clarified the role the Ga wetting layer plays in rf plasma molecular beam epitaxy of GaN when Mg doping, for [Mg] from $\sim 2\times10^{19}$ to $\sim 1\times10^{20}$ cm^{-3} corresponding to the useful, accessible range of hole concentrations of $p\sim10^{17}$–10^{18} cm^{-3}. Structures were grown in the N-rich and Ga-rich growth regime for single Mg doping layers and for multilayer structures with a range of Mg concentrations. Samples were characterized *in situ* by reflection high-energy electron diffraction and *ex situ* by atomic force microscopy, transmission electron microscopy, convergent beam electron diffraction, and secondary ion mass spectroscopy. Growth on ''dry'' surfaces (without a Ga wetting layer) in the N-rich regime completely inverted to N-face upon exposure to Mg. No reinversion to Ga-face was detected for subsequent layers. Additionally, Mg was seen to serve as a surfactant during this N-rich growth, as has been reported by others. Growth initiated in the Ga-rich regime contained inversion domains that nucleated with the initiation of Mg doping. No new inversion domains were found as the Mg concentration was increased through the useful doping levels. Thus the Ga wetting layer was found to inhibit nucleation of N-face GaN, though a complete wetting layer took time to develop. Finally, by establishing a complete Ga wetting layer on the surface prior to growth, we confirmed this finding and demonstrated Mg-doped GaN completely free from inversion domains to a doping level of $[\mathrm{Mg}]\sim2\times10^{20}$. © *2003 American Vacuum Society.*
[DOI: 10.1116/1.1589511]

I. INTRODUCTION

p-type doping of gallium nitride is critical for many electronic and optoelectronic applications. The advent of readily achievable *p*-type GaN by Mg doping in metalorganic chemical vapor deposition (MOCVD) led to the emergence of the nitride semiconductor field and the predominance of the MOCVD growth technique.[1] While the development of molecular beam epitaxy (MBE) has lagged the development of MOCVD, there are some advantages seen in MBE of GaN, and Mg-doped GaN in particular. Mg doping in MBE has achieved equivalent electrical characteristics when compared to MOCVD grown material without the necessity of a postgrowth activation anneal. Further, Mg doping in MBE is shown to yield sharp interfaces and not suffer from the Mg memory effect present in MOCVD.[2] Finally, MOCVD growth of Mg-doped GaN is seen to lead to saturation in hole concentration, potentially related to formation of Mg precipitates.[3,4] The formation of Mg precipitates has not been observed in MBE grown GaN.

MBE growth of unintentionally doped (UID) GaN has advanced through the study of the growth or surface phase diagram, which includes three regions of growth conditions. The three conditions for growth include N-rich (III/V$<$1), Ga-rich (III/V$\sim$1) ''intermediate,'' and Ga-rich (III/V$>$1) with excess droplet formation.[5,6] The boundaries between these regions are seen to be a function of substrate temperature, and are shown for a fixed nitrogen flux in Fig. 1.[7] Additionally, the surface coverage of Ga is found to evolve during growth and depends on the amount of Ga excess supplied to the surface. So, while the III/V ratio supplied to the surface may be Ga rich, a complete Ga wetting layer requires time to buildup. Studies of unintentionally doped GaN have established metal rich growth conditions as essential for high quality material. N-rich growth conditions lead to facetted surface morphologies and increased trap states. The role of the Ga wetting layer has been found to be crucial to both structural quality as well as reduced impurity incorporation.[8,9] Control of the Ga wetting layer has also recently been found feasible through *in situ* measurement of reflection high-energy electron diffraction (RHEED).[10]

Studies of Mg-doped GaN growth by rf-plasma MBE started with investigations of the effect of substrate temperature and Mg flux. Guha *et al.* found the Mg to have a saturation concentration in GaN as function of substrate temperature, with higher saturation concentrations available for lower growth temperatures.[11] Several groups have also re-

[a)]Electronic mail: speck@mrl.ucsb.edu

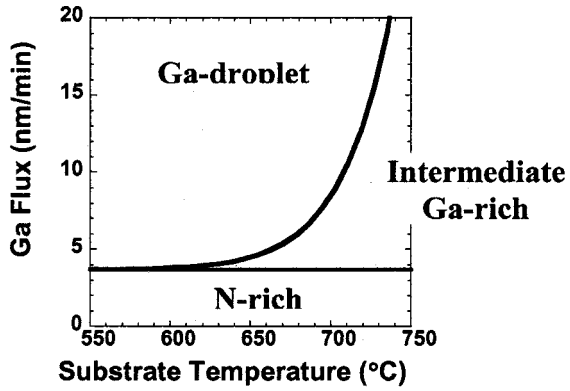

FIG. 1. GaN growth diagram illustrating different surface condition regimes as a function of substrate temperature and Ga flux for a fixed nitrogen flux.

ported linear incorporation of Mg below the flux required for saturation.[12,13] Further, for a given Mg flux, the incorporated Mg concentration increases exponentially for a decrease in substrate temperature. The finding of the saturated incorporation rate suggested that Mg incorporation takes place via a surface phase accumulation or via particular crystal sites. The next studies looked at the influence of the surface III/V ratio on crystal quality. Haus *et al.* found that while the III/V ratio did not affect Mg incorporation, the surface condition did strongly affect electrical characteristics. Samples grown in the Ga-rich and intermediate region had measurable Hall mobilities, while the N-rich samples were seen to be resistive. Optimal films resulted for conditions of Ga-rich growth close to the boundary of the droplet formation regime at a substrate temperature of 650 °C.[7] This optimization balances the need to lower the substrate temperature to increase Mg incorporation and the need to raise the substrate temperature to reduce incorporation and/or formation of compensating defects such as oxygen and nitrogen vacancies. Films have been achieved with [Mg] from $\sim 2\times10^{19}$ to $\sim 1\times10^{20}$ cm^{-3}, which corresponds to the useful, accessible range of hole concentrations of $p\sim10^{17}-10^{18}$ cm^{-3}.[2] This optimal temperature for p-type GaN is lower than the optimal temperature for n-type GaN. Improved n-type GaN films and AlGaN/GaN heterostructures have been grown with substrate temperatures closer to 750 °C.[6,14] The higher sticking coefficient of Si enables these films to benefit from reduced impurity incorporation at higher growth temperature. These same compensation mechanisms are present in MOCVD growth of GaN:Mg, with the exception that formation of Mg–H complexes, common in MOCVD, is not a consideration for rf-plasma MBE growth.[3]

Surprisingly, the typical GaN (0001) crystal polarity will invert during MBE growth of Mg-doped GaN under some conditions. Ramachandran *et al.* first remarked upon polarity inversion due to Mg doping while growing in a nitrogen rich growth regime.[15] This complete inversion along the (0001) basal plane was reported to result from exposing the surface to 1.2 ± 0.4 ML of Mg or more, under Ga poor growth conditions. The inversion domain boundary was observed in transmission electron microscopy (TEM) and the polarity was confirmed by convergent beam electron diffraction (CBED). The inverted material was noted to exhibit, upon cooling below ~300 °C, higher order RHEED reconstructions of (3×3), (6×6), and $c(6\times12)$ for increasing Ga coverage rather than the typical (1×1) and (2×2) for Ga-face GaN. The inversion was argued to result from the formation of Mg_3N_2 at the inversion domain boundary based on energetic calculations. Romano *et al.* and Ptak *et al.* also reported the inversion of GaN with Mg doping.[16,17] Their work associated the formation of inverted material with heavy Mg doping, however, the condition of the III/V ratio was not established. TEM results from this study though reveal inversion domain boundaries along the $\{h,h,-2h,l\}$ planes as well as the (0001) basal plane. This allows the possibility that inversion takes place as a result of Mg atoms occupying threefold-coordinated Ga sites along the $\{h,h,-2h,l\}$ planes.

TABLE I. Summary of sample growth conditions.

Sample list				
Sample	Ga flux (μTorr)	Surface preparation	III/V ratio	Mg layers
A	0.25	none	<1	single
B	0.27	none	<1	single
C	0.31	none	>1	single
D		none	<1	multiple
E		none	>1	multiple
F	0.31	Ga wetting	>1	single

Thus the mechanism and the exact growth regime responsible for polarity inversion have not been fully elucidated. The importance of controlling the polarity is demonstrated by the different electronic and structural properties of GaN films grown under each polarity. Li *et al.* investigated the impact of polarity by changing the nucleation conditions in direct MBE growth on sapphire prior to Mg doping.[18] Li *et al.* found that Mg-doped N-face films have higher defect densities and are more resistive than the p-type films achievable for Ga-face growth. Beyond simply preventing undesirable polarity inversion, understanding the mechanism responsible for inversion allows the potential for controllably changing polarity in a single epitaxial growth.

We present here a study of the growth parameters responsible for Mg inversion especially with respect to the Ga wetting layer that forms during optimal Ga-rich growth conditions.

II. EXPERIMENT

Mg doped GaN films were grown in a Varian Modular Gen II system. The active nitrogen was supplied by an EPI Unibulb rf plasma nitrogen source. Conventional effusion cells were used for Ga and Mg. All samples were grown on ~2 μm thick unintentionally doped ($n\sim4\times10^{16}$) templates of MOCVD-grown GaN (0001) on sapphire. All samples were grown with an rf power of 150 W and a sufficient N_2 flow to maintain a chamber pressure of 1.1×10^{-5} Torr.

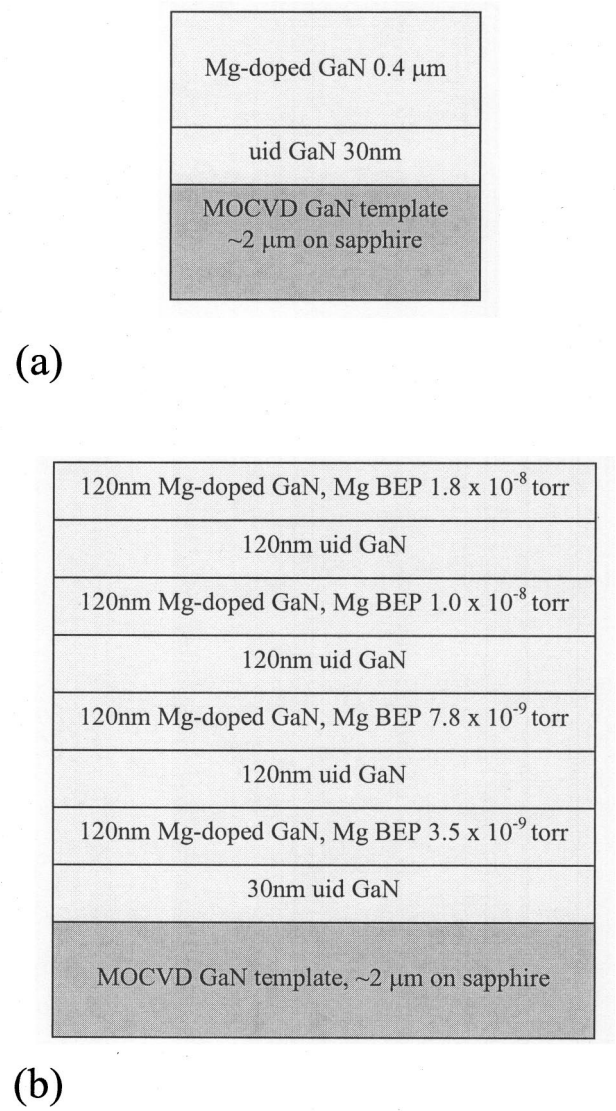

FIG. 2. Schematic of (a) single layer growth structure for samples A–C, and F and (b) multilayer structure of samples D and E, grown N-rich and Ga-rich, respectively.

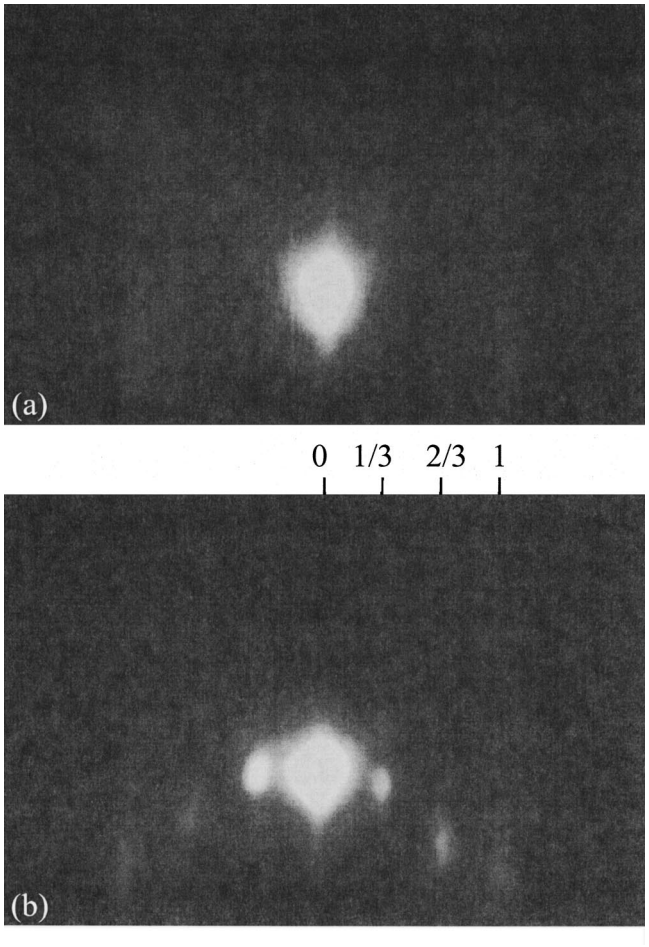

FIG. 3. RHEED patterns along $[2\bar{1}\bar{1}0]$ typical of (a) Ga-face growth and (b) N-face growth exhibiting 3×3 reconstruction (arrows indicate reconstructions).

These conditions correspond to a growth rate of ~200 nm/h or ~0.2 ML/s. The substrate temperature was held at 650 °C for all growths reported here.

The samples were first characterized *in situ* by reflection high-energy electron diffraction (RHEED). RHEED patterns were recorded prior to and postgrowth at growth temperature and upon cooling to a substrate temperature of less than ~250 °C. When possible, RHEED was used to identify the surface polarity at the start and end of growth. Ga-face growth typically exhibits streaky RHEED without reconstructions for Ga-face growth in the absence of arsenic for rf plasma MBE. In contrast, N-face growth will exhibit 3×3 and 6×6 reconstructions upon cooldown depending on the Ga surface coverage. Postgrowth, the Ga surface coverage was monitored by optical microscopy. The Ga-rich samples were observed to have Ga droplets postgrowth, while the N-rich samples were not observed to have any droplets. Subsequently, the samples were etched in HCl to remove excess Ga and the surface morphology was imaged by atomic force microscopy (AFM). Transmission electron microscopy (TEM) was used to look at microstructure and convergent beam electron diffraction (CBED) was used to determine polarity with a JOEL 2000FX electron microscope, operated at 200 kV. The $[1\bar{1}00]$ cross-sectional TEM samples were prepared by polishing and then ion milling. Two beam bright field and weak beam dark field TEM images are taken in $g=0002$ and $g=11\bar{2}0$ diffraction conditions. CBED patterns were taken in the $[1\bar{1}00]$ zone axis. The condenser aperture was 70 μm and the spot size was 40 nm. The contrast of diffraction disks in the CBED pattern is not only dependent on the polarity but also dependent on the sample thickness. Simulation of experimental patterns was carried out by calculating the intensity by the Bloch wave method. The software ''Desktop Microscopist 2.0'' was used for the simulation. The polarity was determined by matching the contrast in central and two {0002} disks between the experimental and simulated patterns. Finally, secondary ion mass spectroscopy (SIMS) was performed on a Physical Electronics 6650

quadrapole dynamic secondary ion mass spectrometer to establish the Mg concentration.

Three sets of samples were prepared to systematically investigate the impact of III/V ratio and Mg flux on polarity and microstructure. The first set of Mg-doped GaN films studied the impact of III/V ratio on the growth of bulk GaN:Mg. The samples consisted of ~400 nm thick Mg-doped GaN that was grown on a 30 nm thick UID GaN buffer. This set consists of samples A, B, and C, which were grown with increasing levels of Ga flux. The Ga beam equivalent pressure (BEP) for samples A, B, and C was 2.5×10^{-7}, 2.7×10^{-7}, and 3.1×10^{-7} Torr, respectively. Samples A and B resulted in N-rich growth, while sample C was in the Ga-rich growth regime.

The second set of samples, labeled D and E, were designed to look at the effect of Mg doping concentration. These two multilayer structures consisted of four alternating layers of UID GaN and Mg-doped GaN with Mg flux increasing from 3.5×10^{-9} to 1.8×10^{-8} Torr—these Mg fluxes correspond to Mg concentrations in the crystals of $\sim10^{19}$–10^{20} cm^{-3} and hole concentrations of $\sim10^{17}$–10^{18} cm^{-3}, respectively, for samples grown under Ga-rich conditions. The Mg fluxes chosen yield Mg exposure rates of $\sim9\times10^{-4}$ to $\sim5\times10^{-3}$ ML/s. We specifically choose this Mg concentration range as it represents the practical range of hole concentrations that can be controllably realized in rf-plasma MBE. Sample D was grown under N-rich conditions and sample E was grown under Ga-rich conditions.

Finally, sample F was grown to clarify the role of the Ga wetting layer. Sample F had the same structure as sample C, with the addition of Ga exposure to the surface prior to growth. This additional step was taken to develop a complete wetting layer prior to growth of the standard structure of a 30 nm UID GaN buffer followed by ~400 nm Mg-doped GaN. The structures are listed below in Table I and shown schematically in Fig. 2.

III. RESULTS AND DISCUSSION

Samples A and B, single Mg-doped GaN layers grown N-rich, were fully inverted. The first indications of inversion were the (3×3) RHEED reconstructions visible upon postgrowth cooldown for both samples. A (3×3) RHEED pattern seen upon cooling below ~250 °C is seen in Fig. 3. TEM images taken in these samples show a clear interface from the start of Mg-doping growth as shown in Fig. 4(a). The interface is not flat; in the high magnification image (not shown) it is faceted. In the range of about 200 nm above the interface no new defects appeared. However, the upper 200 nm thick layer shows highly defective material. $[1\bar{1}00]$ zone axis CBED patterns were taken in the region above and below the interface. Areas of the same thickness were selected to take the CBED pattern, which is realized by taking patterns along the same thickness fringe, in order that the patterns can be compared directly. The inversion of the patterns below and above the interface confirms that the inversion of polarity occurs as shown in Fig. 4(a), and the interface observed is proved to be the inversion domain boundary. The AFM images for these structures indicate different surface morphologies (Fig. 5). Sample A with a lower Ga flux had a locally granular structure that was linked in a fissured formation. Sample B with a slightly higher Ga flux, though still in the N-rich growth regime, was seen to also have a granular local structure though without the connected fissures. Neither sample evidenced step structure. The rms roughness for sample A was 42.2 nm and for sample B was 38.1 nm.

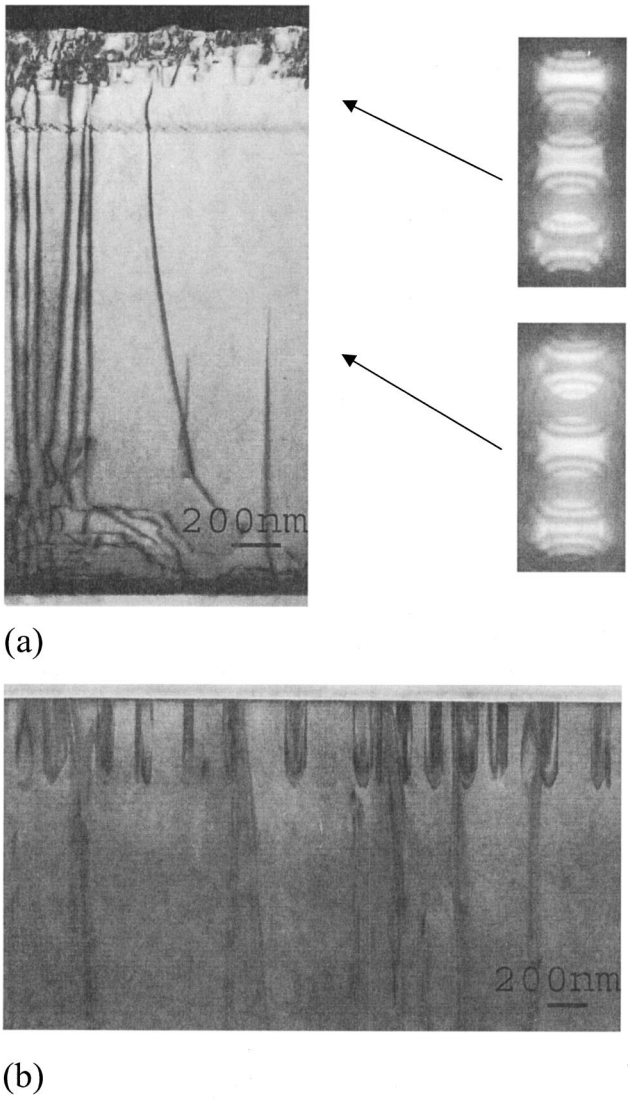

FIG. 4. Cross-section TEM images and CBED patterns of bulk GaN samples grown under (a) N-rich growth of GaN:Mg ($g=[11\bar{2}0]$ dark field, two-beam imaging condition) with CBED patterns taken above and below the interface which show inversion of the diffraction pattern proving inversion of polarity, where the CBED patterns were recorded down the $[1\bar{1}00]$ zone axis and (b) Ga-rich growth of GaN:Mg Ga-rich conditions (bright field, $g=0002$).

Sample C had the same structure as samples A and B but was grown under Ga-rich conditions. Sample C had no obvious initial indication of polarity inversion. The postgrowth RHEED, after cooling below 250 °C, measured on sample C was streaky and only showed a (1×1) pattern (Fig. 3). Droplets were observed on the surface after growth, indicat-

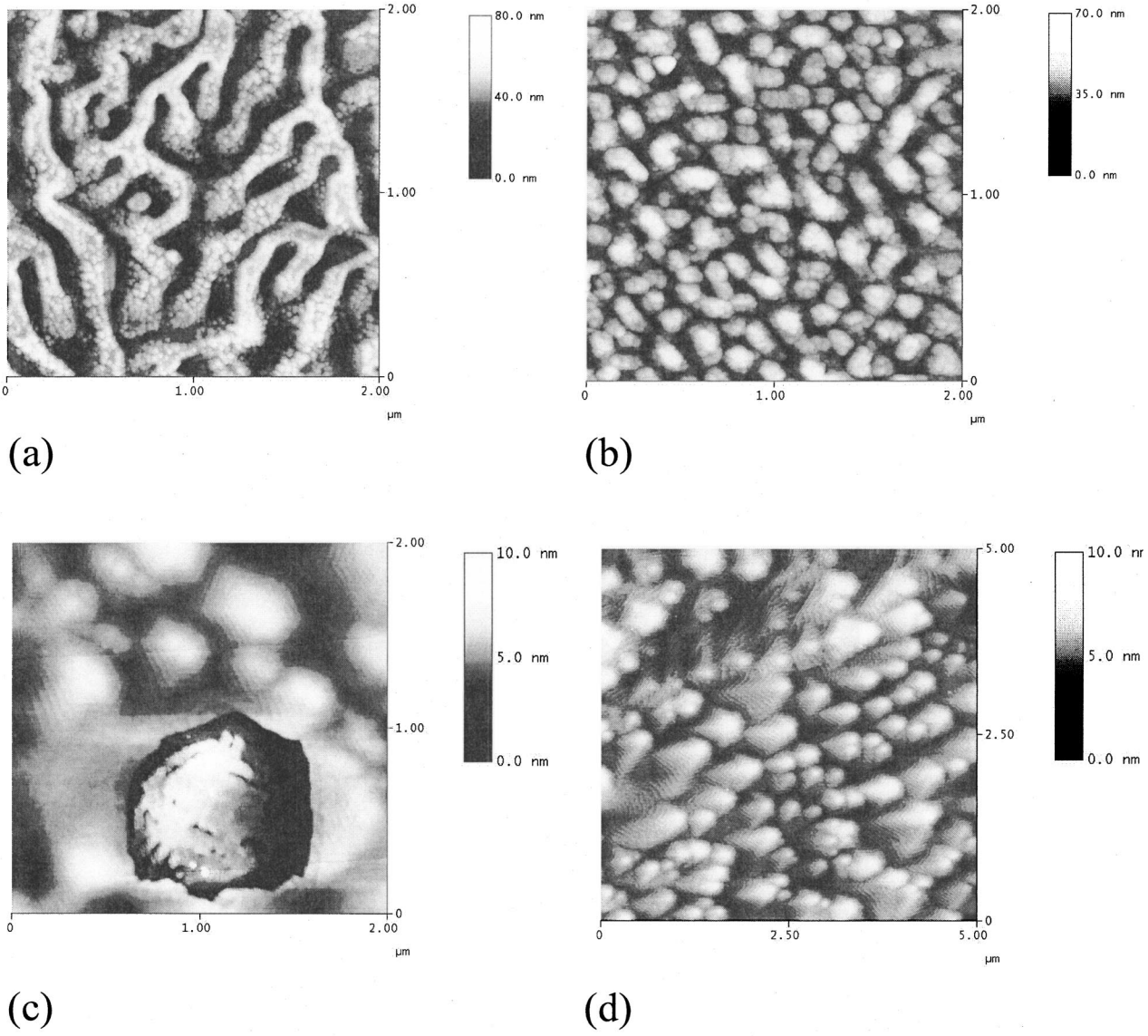

FIG. 5. Surface morphology of (a), (b) N-face GaN for Ga BEP 2.5×10^{-7} and Ga BEP 2.7×10^{-7}, respectively, (c) Ga-face GaN with inversion domains for Ga BEP 3.1×10^{-7}, and (d) inversion domain-free Ga-face GaN for Ga BEP 3.1×10^{-7} with Ga prewet.

ing a complete wetting layer by the end of growth. The AFM images revealed that the surface morphology primarily exhibited spiral step structure mediated by screw-component threading dislocations, typical of Ga-rich MBE GaN.[19] The rms roughness of the surface was also reduced to 10.1 nm. The lower growth temperature yielded GaN films with a tighter spiral morphology. Thus while terraces are clearly defined, the rms roughness value remains high due to the narrow and high spiral growth morphology typical of GaN grown at this temperature. However, the AFM also showed areas with rough morphology markedly different from the surrounding step structure. This rough area appeared locally granular and had a higher height variation similar to the surface morphology of samples A and B. In this sample the interface as observed in samples A and B was not evident, but the faulted structures extending from the growth interface to the surface of the sample were observed as shown in Fig. 4(b). We believe these structures are inversion domains (IDs) though CBED was not able to confirm polarity on these structures. The lateral dimensions of these IDs is much smaller than the rough area on the surface, and are so small as to make them difficult to image in AFM. This suggests that the rough surface morphology is associated with an area of extended defects. Thus while Ga-rich conditions appeared to prevent complete polarity inversion, IDs may still form under Ga-rich conditions.

To investigate the role of Mg concentration, we grew sample D under N-rich conditions with a series of layers of increasing Mg flux. Sample D exhibited the reconstructions typical of N-face material upon postgrowth cooldown. TEM revealed a completely inverted interface at the start of growth. CBED confirmed the polarity inversion and by measuring the CBED through each of the subsequent layers we established that there was no return to Ga-face in this sample

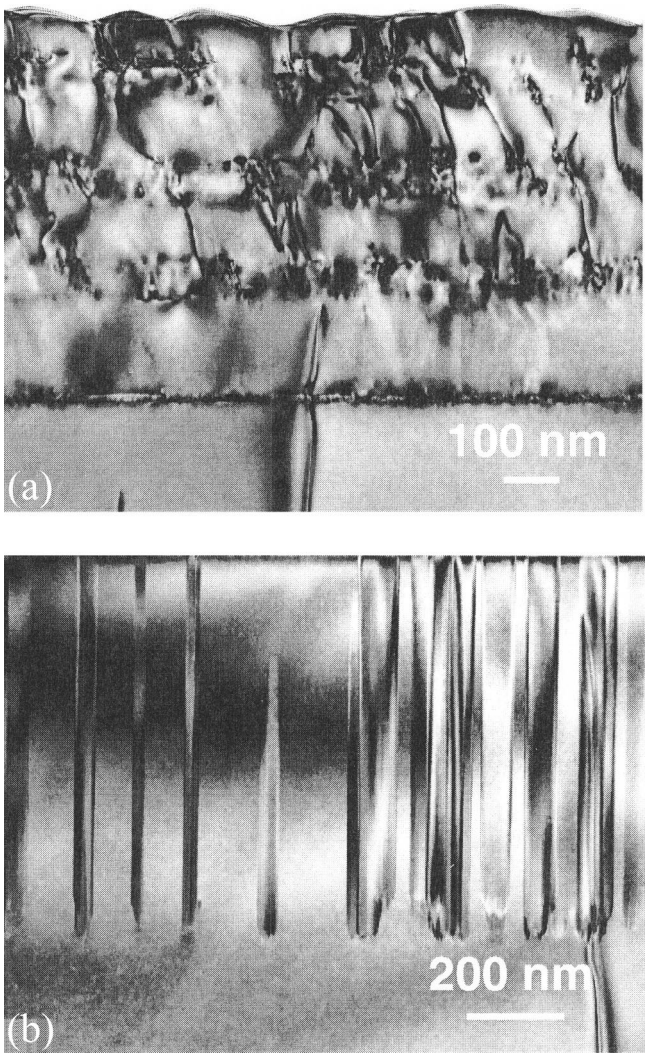

FIG. 6. Cross-section bright field TEM images of a multilayer structure with GaN:Mg layers of increasing Mg flux [see Fig. 2(b) for the growth structure] where (a) was grown in the N-rich regime while (b) was grown Ga-rich (both images were recorded with $g=0002$ two-beam conditions).

through any of the subsequent Mg-doped layers. The TEM clearly shows (Fig. 6) a smoother interface structure for the layers that correspond to the Mg doping. A facetted and rough morphology was clearly evident on the surface. This supports the idea that Mg has a surfactant effect under N-rich growth conditions.[20,21]

Sample E was then grown to look at the impact of Mg doping level under conditions of Ga-rich growth. For this sample, no postgrowth reconstructions were detected. However, similarly to sample C, TEM revealed the presences of what likely are inversion domains. The IDs are seen to generate from the initial growth interface and extend to the surface. However, no new IDs formed for the later Mg-doped layers despite the high Mg flux. These results indicate that while N-rich conditions uniformly lead to polarity inversion, Ga-rich growth only appears to generate inversion domains at growth initiation. This suggests that the formation of the inverted layers depends critically on the local surface state at the growth interface. We then hypothesized the Ga wetting layer has a primary role in preventing ID formation.

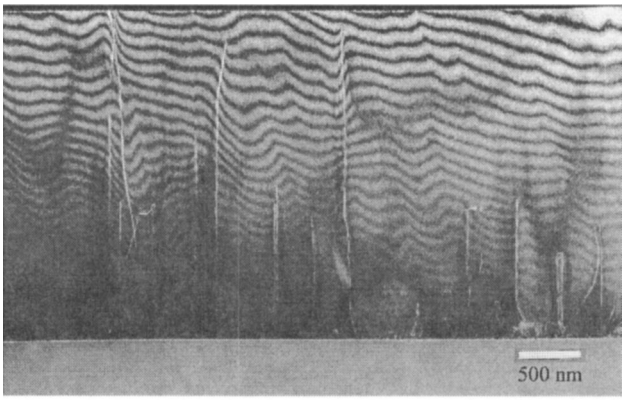

FIG. 7. $g=0002$ dark field cross-section TEM image of an Mg-doped single layer structure with growth initiated with a complete Ga wetting layer.

To confirm this hypothesis, we grew sample F. We repeated the structure of sample C, with the exception that the GaN surface was exposed to a Ga flux prior to growth such that a complete Ga wetting layer was developed. AFM shows a surface morphology free from the inversion domain structures (Fig. 5). The AFM only exhibited step-flow spiral growth and had a rms roughness of 11.1 nm, similar to sample C. Again, the rms roughness was dominated by the presence of narrow, spiral growth structures whose aspect ratio is a result of the lower optimal growth temperature. The absence of the rough, granular areas in this sample indicated the absence of areas of extended defects. Complete suppression of ID formation is confirmed by TEM in Fig. 7. No spike-shaped inversion domains were visible. Also no new extended defects were formed at or above the growth interface. The only threading dislocations present were extended from the underlying GaN template, as is typical for MBE GaN homoepitaxy. This structure was then repeated in a calibration sample to obtain secondary ion mass spectroscopy measurements. A Mg concentration of $\sim 2\times 10^{20}$ cm^{-3} was measured for the calibration sample grown under identical conditions as sample F.

A further consideration concerns whether the inversion is controlled primarily by surface phase or by accumulation of a monolayer of Mg on the surface. To consider this possibility, we revisited sample D and looked at the onset of polarity inversion at the lowest Mg flux. From the TEM we measured the distance from the growth interface to the completion of polarity inversion and after correcting for the buffer region thickness, we estimated the thickness of the region from the beginning of Mg doping to complete inversion to be 30 nm. For the initial Mg flux, assuming a unity sticking coefficient and no incorporation in the growing film (i.e., all Mg incident stays on the surface) we calculated that the thickness needed to accumulate a monolayer of Mg would be 50 nm. This implies that complete inversion occurs even when the Mg on the surface is on the order of $\frac{1}{4}$ to $\frac{1}{2}$ of a monolayer. Given the conservative assumptions of this calculation, we concluded that the presence of a monolayer of Mg on the surface is not requisite for polarity inversion.

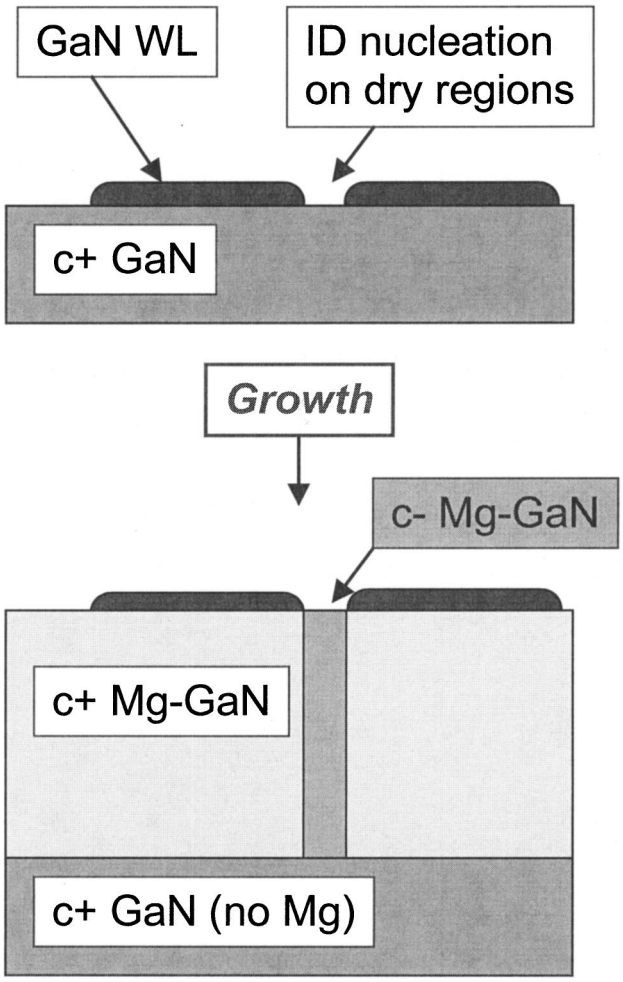

FIG. 8. Model of surface conditions under nominally Ga-rich growth for inversion domain formation.

The results of our experiment clearly indicate that inversion from Ga-face GaN to N-face GaN will take place under conditions of N-rich growth. Additionally, we demonstrate that the formation of inversion domains under Ga-rich conditions is related to a local absence of Ga on the surface. This is clearly demonstrated by the elimination of inversion domains for the sample prewet with Ga prior to growth. The results do not indicate a dependence upon Mg concentration on the surface. We suggest that an inversion domain formation mechanism is dependent upon the surface wetting of Ga as pictured in Fig. 8. Surfaces lacking the Ga bilayer or ''dry'' surfaces appear to provide sites for inversion domain nucleation. Subsequent growth then perpetuates the underlying polarity of the crystal. We have seen no evidence in this work that a return to Ga-face polarity occurs under N-rich or Ga-rich conditions. While the exact mechanism responsible for inversion is still unclear, the role of the Ga wetting layer has been clarified. Several groups have suggested that the formation of Mg_2N_3 is responsible for the polarity switch. The formation of this material has also been reported to allow inversion from the N-face back to the Ga-face.[22] However, we do not find the evidence for Mg_2N_3 formation conclusive.

IV. CONCLUSION

This study has clearly demonstrated that growth of Mg-doped GaN on ''dry'' surfaces, surfaces without a Ga wetting layer, will lead to polarity inversion. Under N-rich growth conditions, we have shown that the completely dry surface will lead to complete polarity inversion. This N-face GaN was never seen to reinvert to a Ga-face. Growth on the N-face was seen to smoothen during Mg-doped layers, confirming the Mg surfactant effect. For Ga-rich growth conditions, inversion domains will nucleate on locally dry surfaces at growth initiation. No further inversion domains will form after a complete Ga wetting layer accumulates, though inversion domains formed at growth initiation extend to the surface. By establishing a complete Ga wetting layer prior to growth, we demonstrated entirely inversion domain-free GaN:Mg growth for Mg concentrations up to $[Mg]\sim 2\times 10^{20}$. There was no evidence of inversion domains nucleating as a result of heavy Mg doping when the Ga wetting layer was present.

ACKNOWLEDGMENTS

The authors would like to thank Tom Mates for his help with the SIMS measurements. This work was supported by ONR (POLARIS MURI, C. Wood program manager). This work made use of the MRL Central Facilities supported by the National Science Foundation under Award No. DMR00-80034. One of the authors (D.S.G.) acknowledges the support of the National Science Foundation Graduate Research Fellowship Program.

[1]S. Nakamura, *The Blue Laser Diode* (Springer, Berlin, 1997).
[2]I. P. Smorchkova, E. Haus, B. Heying, P. Kozodoy, P. Fini, J. P. Ibbetson, S. Keller, S. P. DenBaars, J. S. Speck, and U. K. Mishra, Appl. Phys. Lett. **76**, 718 (2000).
[3]H. Alves, M. Bohm, A. Hofstaetter, H. Amano, S. Einfeldt, D. Hommel, D. M. Hofmann, and B. K. Meyer, Physica B **308**, 38 (2001).
[4]M. Hansen, L. F. Chen, J. S. Speck, and S. P. DenBaars, Phys. Status Solidi B **228**, 353 (2001).
[5]E. J. Tarsa, B. Heying, X. H. Wu, P. Fini, S. P. DenBaars, and J. S. Speck, J. Appl. Phys. **82**, 5472 (1997).
[6]B. Heying, I. Smorchkova, C. Poblenz, C. Elsass, P. Fini, S. Den Baars, U. Mishra, and J. S. Speck, Appl. Phys. Lett. **77**, 2885 (2000).
[7]E. Haus, I. P. Smorchkova, B. Heying, P. Fini, C. Poblenz, T. Mates, U. K. Mishra, and J. S. Speck, J. Cryst. Growth **246**, 55 (2002).
[8]A. Hierro, A. R. Arehart, B. Heying, M. Hansen, U. K. Mishra, S. P. DenBaars, J. S. Speck, and S. A. Ringel, Appl. Phys. Lett. **80**, 805 (2002).
[9]C. Poblenz, T. Mates, M. Craven, S. P. DenBaars, and J. S. Speck, Appl. Phys. Lett. **81**, 2767 (2002).
[10]C. Adelmann, J. Brault, D. Jalabert, P. Gentile, H. Mariette, G. Mula, and B. Daudin, J. Appl. Phys. **91**, 9638 (2002).
[11]S. Guha, N. A. Bojarczuk, and F. Cardone, Appl. Phys. Lett. **71**, 1685 (1997).
[12]D. J. Dewsnip, J. W. Orton, D. E. Lacklison, L. Flannery, A. V. Andrianov, I. Harrison, S. E. Hooper, T. S. Cheng, C. T. Foxon, S. N. Novikov, B. Y. Ber, and Y. A. Kudriavtsev, Semicond. Sci. Technol. **13**, 927 (1998).
[13]J. W. Orton, C. T. Foxon, T. S. Cheng, S. E. Hooper, S. V. Novikov, B. Y. Ber, and A. Kudriavtsev Yu, J. Cryst. Growth **197**, 7 (1999).
[14]C. R. Elsass, C. Poblenz, B. Heying, P. Fini, P. M. Petroff, S. P. DenBaars, U. K. Mishra, J. S. Speck, A. Saxler, S. Elhamrib, and W. C. Mitchel, Jpn.

J. Appl. Phys., Part 1 **40**, 6235 (2001).
[15]V. Ramachandran, R. M. Feenstra, W. L. Sarney, L. Salamanca-Riba, J. E. Northrup, L. T. Romano, and D. W. Greve, Appl. Phys. Lett. **75**, 808 (1999).
[16]L. T. Romano, J. E. Northrup, A. J. Ptak, and T. H. Myers, Appl. Phys. Lett. **77**, 2479 (2000).
[17]A. J. Ptak, T. H. Myers, L. T. Romano, C. G. Van de Walle, and J. E. Northrup, Appl. Phys. Lett. **78**, 285 (2001).
[18]L. K. Li, M. J. Jurkovic, W. I. Wang, J. Van Hove, and P. P. Chow, Appl. Phys. Lett. **76**, 1740 (2000).
[19]B. Heying, E. J. Tarsa, C. R. Elsass, P. Fini, S. P. DenBaars, and J. S. Speck, J. Appl. Phys. **85**, 6470 (1999).
[20]G. Mulal, B. Daudin, C. Adelmann, and P. Peyla, Mater. Res. Soc. Symp. Proc. **595**, W.3.35.1 (1999).
[21]V. Ramachandran, R. M. Feenstra, J. E. Northrup, and D. W. Greve, Mater. Res. Soc. Symp. Proc. **595**, W3.65.1 (1999).
[22]N. Grandjean, M. L. Talent, A. Dussaigne, P. Vennegues, and E. Tournie, IEEE Lasers Electro-Opt. Soc. Proc. **12**, 141 (2002).